Vol. 56: 147–162, 2009
doi: 10.3354/ame01303

AQUATIC MICROBIAL ECOLOGY
Aquat Microb Ecol

Printed September 2009
Published online June 22, 2009

Contribution to AME Special 2 'Progress and perspectives in aquatic primary productivity'

OPEN ACCESS

Comparing electron transport with gas exchange: parameterising exchange rates between alternative photosynthetic currencies for eukaryotic phytoplankton

David J. Suggett[1,*], Hugh L. MacIntyre[2], Todd M. Kana[3], Richard J. Geider[1]

[1]Department of Biological Sciences, University of Essex, Colchester CO4 3SQ, UK
[2]Dauphin Island Sea Lab, 101B Bienville Blvd, Dauphin Island, Alabama 36528, USA
[3]Horn Point Laboratory, 2020 Horns Point Rd, Cambridge, Maryland 21613, USA

ABSTRACT: Estimates of aquatic primary productivity derived from *in situ* active chl *a* fluorescence have rapidly gained popularity over the past 2 decades. This trend has been driven primarily by the need to improve upon 'conventional' carbon (C) uptake- or oxygen (O_2) evolution-based productivity estimates that require water samples to be incubated *ex situ*. Unlike the conventional approaches to measuring productivity, chlorophyll fluorescence measurements inherently describe only the activity of photosystem II (PSII) in the light reactions; thus, the photosynthetic 'currency' of the fluorescence-based approach is an electron turnover rate for PSII (ETR_{PSII}). A photosynthetic currency of electrons has limited ecological relevance but can be converted to a currency of carbon if an 'exchange rate', i.e. a value or factor of equivalence for any single time point, is applied. We used fast repetition rate fluorometry (FRRf), mass inlet membrane spectrometry (MIMS) and ^{14}C uptake to determine ETR_{PSII}, gross and net O_2 evolution and C fixation measured simultaneously for 6 microalgal species and for different steady-state growth conditions. Quantifying the PSII reaction centre (RCII) concentration and the spectral dependency of the effective absorption cross section yielded an FRRf approach that provided a robust estimate of the ETR_{PSII} and gross O_2 evolution for all species and conditions tested; however, the ETR_{PSII} exceeded carbon dioxide (CO_2) uptake by a factor of ~5.4 to 11.6. At least 3 species exhibited substantial light-dependent O_2 cycling to account for ~40 to 60% of the difference between the ETR_{PSII} and CO_2 uptake. The highly variable nature of the ETR_{PSII}:CO_2 uptake 'exchange rate' observed here highlights the need for future studies that rely on active fluorescence to examine aquatic productivity to focus towards a systematic description of how electrons are coupled to C fixation in nature.

KEY WORDS: Fast repetition rate fluorescence · Electron transport · Photosynthesis · Oxygen evolution · Carbon uptake · Phytoplankton

INTRODUCTION

Photosynthesis involves numerous pathways. In the case of oxygenic phototrophs, this involves evolution of oxygen (O_2) from water (H_2O) by the 'light reactions' and uptake of carbon dioxide (CO_2) by the 'dark reactions'; thus, both O_2 and CO_2 represent the primary 'currencies' by which photosynthesis operates. Tracing O_2 evolution and/or CO_2 uptake has long been the convention for quantifying photosynthesis rates. Thus, considerable effort has been invested in optimising tracer techniques since their introduction in the 1950s (Steeman Nielsen 1952), particularly for phytoplankton, which represent the most widespread and diverse group of the aquatic phototrophs and account for the majority (95%) of global aquatic productivity. Attempting to reconcile productivity measurements between studies that have focused on either O_2 evolution or CO_2

*Email: dsuggett@essex.ac.uk

fixation has often proven to be problematic since a number of pathways that uncouple the 2 processes operate. The net evolution of O_2 and net uptake of CO_2 reflect the combination of pathways that produce and compete for energy (ATP) and reductant (NAD(P)H).

Oxygen is evolved only through photosynthetic hydrolysis at the photosystem II (PSII, Table 1) reaction centre complex, but is consumed within the cell via various pathways (Lewitus & Kana 1995, Beardall et al. 2003, Behrenfeld et al. 2008); this minimises accumulation of toxic O_2 molecules, as well as disposing of excess reductant and ATP that would otherwise constrain optimal photosynthetic activity (Beardall et al. 2003, Behrenfeld et al. 2004). Consumption of O_2 in the light can occur through a number of processes: (1) photoreduction of O_2 via reduced electron transport components associated with PSI, known as the Mehler Reaction, which consumes reductant (Badger et al. 2000); (2) photoreduction of O_2 via alternative terminal oxidases located in the thylakoid membranes (McDonald & Vanlerberghet 2006, Bailey et al. 2008, Cardol et al. 2008, Mackey et al. 2008); (3) light-enhanced mitochondrial respiration linked to ATP synthesis (Xue et al. 1996); (4) light-enhanced mitochondrial respiration through the alternative oxidase (AOX) without pumping protons across the inner mitochondrial membrane (McDonald & Vanlerberghet 2006) and (5) oxygenase activity of ribulose bisphosphate carboxylase/oxygenase (rubisco) (Badger et al. 2000, Beardall et al. 2003). Unfortunately, operation of these various pathways is neither well characterised nor quantified for many key phytoplankton or growth conditions.

Carbon dioxide is fixed into organic matter (i.e. reduced with consumption of NADPH) by carboxylation of ribulose biphosphate (RuBP) in the Calvin cycle. After carboxylation by rubisco, the major CO_2 uptake processes are anaplerotic β-carboxylations, which provide essential intermediates that cannot be produced from the Calvin-Benson cycle, and may also play a role in C_4 photosynthesis in diatoms (Reinfelder et al. 2000, Roberts et al. 2007). However, CO_2 is also produced from mitochondrial respiration of organic matter and as a product of photorespiration. Gross photosynthesis is defined as the rate of evolution of O_2 by PSII, and/or the rate of CO_2 fixation, almost entirely by the Calvin cycle. Gross photosynthetic O_2 evolution can be measured with little or no ambiguity by using the tracer ^{18}O either directly as the rate of ^{18}O and ^{16}O evolution from a mixture of $H_2{}^{18}O$ and $H_2{}^{16}O$ (Bender et al. 1987), or indirectly as the sum of net O_2 evolution and gross O_2 consumption, where consumption is determined from the rate of decline in $^{18}O_2$ (Kana 1990). The most common method for estimating gross CO_2 fixation is to follow the uptake of $^{14}CO_2$ into particulate and dissolved organic matter, which approximates gross photosynthesis when the respiration rate is low and incubations are short. However, the measured rate of $^{14}CO_2$ fixation may underestimate gross photosynthesis due to isotope disequilibrium between the intracellular and extracellular CO_2 pools (reviewed by MacIntyre & Cullen 2005).

For many studies employing measurements of net gas exchange, only net photosynthesis (the balance between gross O_2 evolution in photosynthesis and its consumption in all respiratory pathways) can be compared with CO_2 uptake. Such comparisons yield the photosynthetic quotient (PQ), which is the ratio of the moles of O_2 produced per mole of CO_2 assimilated. Variability in the PQ demonstrates that the relationship between these 2 primary currencies is not constant, but instead depends upon the redox state of the substrate used for growth, par-

Table 1. Terms and definitions used throughout the main text. Note that the prime refers to fluorescence measurements made under actinic (background) light while unprimed terms refer to measurements made under dark acclimated conditions. Units are dimensionless unless otherwise specified

Term	Definition
PSII	Photosystem II
RCII	PSII reaction centre concentration, RCII m^{-3}
ϕ_{PSII}	Quantum yield of PSII photochemistry, $Å^2$ quantum^{-1}
ϕ_{RC}	Quantum yield of RCIIs, mol e^- [mol photon]$^{-1}$
ϕ_e	Quantum yield of electron transfer, mol e^- [mol O_2]$^{-1}$
ETR_{PSII}	Electron transfer rate of PSII, mol e^- [mol chl *a*]$^{-1}$ min^{-1} (Eq. 2)
Chl *a*	Concentration of chl *a*, mg m^{-3}
E	(=PFD) Light intensity, µmol photons m^{-2} s^{-1}
E_k	*E* required to saturate photosynthesis, µmol photons m^{-2} s^{-1}
a_{PSII}	Absorption coefficient for photochemistry solely through PSII, m^{-1}
a_{PSII}^*	Chl *a*-specific PSII absorption coefficient, m^2 [mg chl *a*]$^{-1}$
F_{730}	Fluorescence excitation yield (with emission set to 730 nm)
$1/n_{PSII}$	Photosynthetic unit size of PSII, mol chl *a* [mol RCII]$^{-1}$
F_o (′)	Minimum fluorescence yield under dark acclimation (actinic light)
F_m (′)	Maximum fluorescence yield under dark acclimation (actinic light)
F'	Fluorescence yield at any point between F_o' and F_m'
F_v/F_m	Potential photochemical efficiency of open RCIIs = $(F_m - F_o)/F_m$
F_q'/F_v'	PSII efficiency factor under actinic light = $(F_m' - F')/(F_m' - F_o')$ = qP
F_v'/F_m'	Photochemical efficiency of PSII under actinic light =$(F_m' - F')/F_m'$
F_q'/F_m'	Maximum efficiency of PSII under actinic light = $(F_m' - F_o')/F_m'$
σ_{PSII} (′)	Effective absorption cross section of PSII under dark acclimation (actinic light), m^2 [mol RCII]$^{-1}$
ρ (′)	RCII connectivity under dark acclimation (actinic light)
$\overline{\sigma_{PSII}}'$	Effective absorption cross section of PSII spectrally weighted to a specific actinic light source

ticularly the nitrogen source (e.g. nitrate vs. ammonium; Williams et al. 1979), or the end-products of catabolism (e.g. Laws 1991). However, the PQ represents an important tool for photobiology: it not only provides a potentially convenient means of examining how cells invest photochemical energy for growth, but it is also an effective physiological 'exchange rate' that can be used to interconvert between commonly measured photosynthetic currencies.

Electrons as photosynthetic currency

Active fluorometry, which measures changes in chl *a* fluorescence yield of PSII, is an alternative approach to measuring primary productivity that was introduced to aquatic research in the 1990s. It provides a direct optical measure of the efficiency with which absorbed light is used for PSII photochemistry (e.g. Krause & Weis 1991). Because electron flow out of PSII requires oxidation of water to O_2, active fluorescence should provide an alternative measure of the true gross O_2-evolving potential of the photosynthetic organism (Genty et al. 1989). Two techniques of active fluorometry are currently used: pulse amplitude modulated (PAM; Schreiber et al. 1993) fluorometry and fast repetition rate fluorometry (FRRf; Kolber et al. 1998). Both measure PSII photochemical efficiency (ϕ_{PSII}, Table 1); however, FRRf has some advantages over PAM, including simultaneous measurements of the effective absorption by PSII (σ_{PSII}; Falkowski et al. 1986, Kolber et al. 1988), and *in situ* deployment combined with the high sensitivity required to examine the lowest chlorophyll concentrations in oligotrophic water masses (Kolber & Falkowski 1993, Babin et al. 1996). With these additional capabilities, the FRR fluorometer became the 'oceanographer's choice' for phytoplankton studies.

Early studies demonstrated that measurements of ϕ_{PSII} could be closely related to measurements of the quantum yield of O_2 evolution (e.g. Falkowski et al. 1986, Flameling & Kromkamp 1998). With additional knowledge of the rate of light absorption, which depends on the incident photon flux density and the absorption cross section, ϕ_{PSII} can be used to calculate productivity. The absorption cross section must be specific to light harvesting for photochemistry through PSII (a_{PSII}, Table 1); here, productivity is strictly the electron transfer rate by PSII (ETR_{PSII}; Kromkamp & Forster 2003, Suggett et al. 2003):

$$ETR_{PSII} = E \times a_{PSII} \times \phi_{PSII} \quad (1)$$

where E is light intensity (µmol photons m^{-2} s^{-1}); a_{PSII} is the absorption coefficient for photochemistry solely through PSII (m^{-1}); and ϕ_{PSII} is the quantum yield of PSII (Å^2 quantum^{-1}).

Later studies included additional measurements of absorption, enabling ETR_{PSII} to be compared with corresponding photosynthesis rates obtained via O_2 evolution (Beer et al. 1998, Franklin & Badger 2001, Suggett et al. 2001) and C uptake (Kolber & Falkowski 1993, Boyd et al. 1997, Hartig et al. 1998). These studies were a critical step for estimates of primary productivity since, unlike gas exchange measurements, fluorescence-based rates could be measured optically, *in situ* and extremely rapidly (µs to ms), i.e. without the need to incubate and sacrifice material. Therefore, the use of active fluorescence introduced another photosynthetic 'currency' to productivity studies — that of electrons. However, the 'exchange rates' required to interconvert between the currency of electrons and the more conventional currencies of CO_2 or O_2 are still not well characterised. There remains a vital need to compare primary productivity data sets derived from these different methodologies.

Comparing FRRf with O_2- and C-based photosynthesis rates

The growing use of FRRf has been accompanied by comparisons of FRRf-based ETRs with 'conventional' measures of phytoplankton productivity (Table 2). Most comparisons are between FRRf and ^{14}C methods, although a few studies of natural systems have used O_2 techniques. The reported ratios of ETR_{PSII}:CO_2 uptake are highly variable, ranging from 2.5 to 12 mol e^- [mol CO_2]$^{-1}$, which is an approximately 5-fold range in the currency conversion 'rate'. A reference ratio is usually set at 4, based on the minimum number of PSII electrons derived from 2 water molecules in the production of 1 O_2 molecule. While it is difficult to reconcile measured ratios <4, it is possible that ratios >4 could be related to alternative physiological electron sinks ((Lewitus & Kana 1995, Badger et al. 2000, Beardall et al. 2003), electron cycling around PSII (Prášil et al. 1996) and/or electron slippage back to the water oxidizing complex (Quigg et al. 2006). We have been unable to reconcile variability in the ratio by classifying the data in Table 2 according to the dominant taxonomic components or environmental regimes ($p > 0.05$, using SIMPER test in PRIMER-E), so it is appropriate to consider methodology as a source of the variance.

Measures of FRRf (ETR_{PSII}) and gas exchange data differ in terms of the timescale and the manner in which the water sample is handled. Specifically, FRRf measurements of photosynthetic parameters are obtained on a microsecond timescale, although averaged data from several individual measurements are used in practice (e.g. Corno et al. 2005, Suggett et al. 2006b).

Table 2. Comparisons of primary productivity estimated using fast repetition rate (FRR) or pump and probe (PP) fluorescence electron transfer rates (ETR_{PSII}) vs. that estimated using carbon uptake or oxygen evolution. Comparisons are based on simulated *in situ* (SIS) and photosynthesis–irradiance (PE) light-response curves. Data sets within each publication have been grouped according to the predominant taxonomic group to yield a single value for the ratio between the rates of electron transport (mol e^- [g chl *a*]$^{-1}$ h^{-1}) and C uptake (mol CO_2 [g chl *a*]$^{-1}$ h^{-1}) or O_2 evolution (mol O_2 [g chl *a*]$^{-1}$ h^{-1}). In each case, the predominant sampling conditions (time of year, location) are also given. Data were digitised where necessary by scanning the original material and processing through DigitizeIt v1.5 software; the regression (and coefficient of determination, r^2) between productivity 'currencies' were recalculated with a 0 intercept. Note that the data of Fujiki et al. (2007) were recalculated using values for photosynthetic unit size of PSII ($1/n_{PSII}$) reported here and values for effective absorption cross section of PSII under dark acclimation (σ_{PSII}) that were adjusted to spectrally weight the fluorometer response to the white light-emitting diodes (LEDs) used for ^{14}C-uptake incubations. *E*: (=PFD) light intensity, µmol photons m^{-2} s^{-1}, LD: light–dark, n/a: not available, NS: not significant

Techniques	Approach	Ratio	r^2	Dominant group	Location/timing	Source
PP vs. C	*In situ* vs. SIS 4 h PE	5.44: 1	0.78	n/a	NW Atlantic, various	Kolber & Falkowski (1993)
(mol e^-: mol CO_2)	*In situ* vs. 2 h PE	2.45: 1	0.13	Coccolithophores	NE Atlantic, summer	Boyd et al. (1997)
FRR fluorescence	*In situ* vs. 1 h PE	8.66: 1	0.59	Cyanobacteria, small flagellates	NE Atlantic, spring	Suggett et al. (2001)
vs. C	*In situ* vs. 1–2 h PE	6.03: 1	n/a	Diatoms, dinoflagellates	UK shelf, summer	Moore et al. (2003)
(mol e^-: mol CO_2)		3.94: 1	n/a	Coccolithophores, flagellates		Moore et al. (2003)
	In situ vs. 1–2 h PE	11.9: 1	n/a	Diatoms, dinoflagellates	Baltic Sea, spring	Raateoja et al. (2004)
		8.81: 1	n/a	Cyanobacteria, flagellates		Raateoja et al. (2004)
	In situ vs. SIS 24 h PE	2.98: 1	NS	Coccolithophores, flagellates	UK shelf, late spring	Smyth et al. (2004)
	In situ vs. SIS (day) PE	8.81: 1	0.94	Picoeukaryotes, prochloropytes	Pacific Ocean, annual	Corno et al. (2005)
	In situ vs. 2 h PE	9.09: 1	0.89	Diatoms, small flagellates	W Atlantic, late spring	Estévez-Blanco et al. (2006)
	In situ vs. SIS 3 h PE	4.60: 1	0.88	Diatoms, Cyanobacteria	Alpine lake, annual	Kaiblinger & Dokulil (2006)
	In situ vs. 1 h PE	4.13: 1	0.81	n/a	Coastal US (NE), annual	Melrose et al. (2006)
	In situ vs. SIS 24 h PE	10.1: 1	0.48	Coccolithophores, flagellates	UK shelf, late spring	Pemberton et al. (2006)
	In situ vs. *in situ* pH	4.04: 1	0.86	Diatoms	UK lake, spring	Suggett et al. (2006a)
		6.12: 1	0.62	Diatoms, flagellates		Suggett et al. (2006a)
	In situ vs. SIS (day) PE	7.08: 1	n/a	Picoeukaryotes, cyanobacteria,	Tropical Atlantic various	Suggett et al. (2006b)
		16.9: 1	n/a	Prochloropytes, picoeukaryotes	Atlantic gyres, various	Suggett et al. (2006b)
	In situ vs. 1 h PE	4.36: 1	0.89	Cyanobacteria, flagellates	US Great Lakes, late summer	Pemberton et al. (2007)
	In situ vs. 2 h PE	9.68: 1	n/a	Cyanobacteria, chlorophytes	Netherlands lake, summer	Kromkamp et al. (2008)
	Step PE (5 min E^{-1}) vs. 20 min PE	6.08: 1	0.88	*Dunaliella tertiolecta*	Laboratory-based	Fujiki et al. (2007)
FRR fluorescence	*In situ* vs. LD bottles	12.0: 1	0.88	Cyanobacteria, small flagellates	NE Atlantic, spring	Suggett et al. (2001)
vs. O_2	*In situ* vs. triple isotope	2.52: 1	NS	n/a	E Japan, May–June	Sarma et al. (2005)
(mol e^-: mol O_2)	*In situ* vs. LD bottles	3.95: 1	NS	n/a		Sarma et al. (2005)

This gives a 'snapshot' that may or may not be an accurate representation of the average condition during an incubation that is long enough to quantify gas exchange. The relationship between the ETR and gas exchange will also depend on the nature of the incubation (e.g. *in situ*, simulated *in situ*, or within a photosynthetron), which determines the irradiance field and may cause photosynthetic regulation within the gas exchange experiments that would not be captured by the FRRf measurement (MacIntyre et al. 2000): photosynthetic rates measured over short timescales (s to min) integrate only relatively rapid physiological adjustments to the environment, such as xanthophyll cycle activity and state transitions, while those measured over longer timescales (h) integrate relatively slow processes, such as photoinhibition, pigment turnover and protein synthesis (MacIntyre et al. 2000).

A related methodological issue is the need to measure or estimate the rate of photon absorption by PSII, a_{PSII} (Eq. 1). In FRRf studies, a_{PSII} is obtained from the effective absorption of PSII, σ_{PSII} (m^2 [mol RCII]$^{-1}$), which is derived directly from the FRR fluorescence rise kinetics (Kolber et al. 1998). Importantly, σ_{PSII} is weighted to the spectral quality of light used to induce the fluorescence transient (i.e. the flash lamp or light-emitting diode, LED, in the fluorometer) and thus must be corrected to the spectrum of the ambient irradiance that drives photosynthesis (Suggett et al. 2001, Raateoja et al. 2004, MacIntyre & Cullen 2005). The correction cannot be made without spectral light data or the spectral absorption of PSII (Melrose et al. 2006, see also Suggett et al. 2006b). Converting values of ϕ_{PSII} to a_{PSII} requires knowledge of the reaction centre (RCII) concentration, which is difficult to quantify (Kolber & Falkowski 1993, Babin et al. 1996, Suggett et al. 2001). Typically, studies have either assumed the RCII concentration to be constant (e.g. Raateoja et al. 2004, Kromkamp et al. 2008), or have applied a 'functionality' factor (Kolber & Falkowski 1993, Babin et al. 1996, Suggett et al. 2001). Neither approach appears to yield a satisfactory approximation of the actual RCII concentration (Suggett et al. 2004) unless the phytoplankton community structure remains relatively constant (Suggett et al. 2006a, see also Moore et al. 2006).

Although FRR-type fluorometers have been commercially available for more than a decade, only 2 studies have compared FRRf-based ETRs with 'conventional' photosynthesis measurements for phytoplankton grown in the laboratory (Suggett et al. 2003, Fujiki et al. 2007; Table 1). Unfortunately, neither of these studies included measurements of the RCII concentration. Therefore, the aim of this investigation was to determine how closely FRRf-based measures of ETR_{PSII} relate to (1) gross O_2 evolution and (2) C fixation rates of phytoplankton under defined growth conditions. For the first time, we compare these 'currencies' using measurements made synchronously on the same sample and, in the case of ETR_{PSII} do not include assumptions of RCII concentration or spectral dependency of σ_{PSII}, but rather directly measure these factors.

MATERIALS AND METHODS

Cell growth. Measurements were performed on 6 species representing key eukaryotic microalgal groups: *Dunaliella tertiolecta* (Chlorophyceae); *Pycnococcus provasolii* (Prasinophyceae); *Storeatula major* (Cryptophyceae); *Aureococcus anophagefferens* (Pelagophyceae); *Thalassiosira weissflogii* (Bacillariophyceae); and *Prorocentrum minimum* (Dinophyceae). Cells were grown at 20°C in 1.5 l semi-continuous culture bubbled with air (MacIntyre & Cullen 2005). The medium was artificial seawater (Keller et al. 1987). Salinity was adjusted to 30 for all species except for *Prorocentrum minimum* and *Storeatula major*, for which it was reduced to 15. The medium was enriched with f/2 levels of nitrate, phosphate, trace metals and vitamins (Guillard & Ryther 1962), plus 107 µM silicate (Guillard 1975) and 10 nM H_2SeO_3 (Keller et al. 1987). Cultures were grown under continuous illumination from cool-white fluorescent lamps (Osram Sylvania F15T8-CW) at photon flux densities (PFDs) of 18, 80 and 300 µmol photons m^{-2} s^{-1}, with the exception of *A. anophagefferens* and *T. weissflogii* for which only the low- and mid-growth PFDs (18 and 80 µmol photons m^{-2} s^{-1}) were possible. Specific growth rates (Table 3) were estimated from daily measurements of chl *a* concentration, which was determined using the non-acidification technique (Welschmeyer 1994) after extraction in dimethyl sulfoxide and 90% acetone (Shoaf & Lium 1976). Cells were harvested at the exponential growth phase.

Experimental set up. A Fast^{tracka} FRR fluorometer (Chelsea Instruments) was immersed in water maintained at 20°C. Four gas-tight glass tubes were filled (~8 ml to leave 0 headspace) with culture that had been enriched either with $^{18}O_2$ or $NaH^{14}CO_3$ (see below). The tubes were then stacked horizontally in a vertical array over the fluorometer's optical head, alternating the treatments. The bottom-most tube, which sat directly in front of the fluorometer's excitation-emission window, was always one that was enriched with $^{18}O_2$, enabling measurements of fluorescence yield and ^{18}O uptake on the same sample. Actinic illumination was provided at 90° to the fluorometer's excitation window by a slide projector equipped with a dispersing lens. Light from quartz halogen bulbs (General Electric ENH) was filtered

through a 2.5 cm layer of 10 g l^{-1} of $CuSO_4$ (aq.) and illuminated the entire stack of tubes.

Parallel measurements of active fluorescence and gas flux were made on each sample at 3 different actinic PFDs: 35 to 75, 185 to 385 and 615 to 1200 µmol photons m^{-2} s^{-1} (designated low, medium and high hereafter). These corresponded to a factor that was 0.06 to 17.0 times the irradiance required to saturate photosynthesis, E_k, as determined from parallel ^{14}C-based photosynthesis– irradiance curves (following MacIntyre et al. 1996; see also the method for C uptake described below), with the exception of one value (54.1) for *Aureococcus anophagefferens* (Table 3). The PFD was measured in front of the glass tubes after each set of incubations using a Biospherical QSL-101 scalar quantum irradiance sensor (Biospherical Instruments). The duration of the incubations was reduced with the increase in actinic PFD from 50 to 60 min (low), to 40 – 50 (medium) and 20 to 30 min (high), to prevent the formation of bubbles within the tubes while maintaining favorable signal: noise ratios (SNR) with the fluorometer.

FRR fluorometry. Single-turnover (ST) FRR fluorescence measurements consisting of 100 flashlets of 1.1 µs duration were made every 2 to 3 s, following Suggett et al. (2003, 2004) throughout the illumination period and in the dark immediately after illumination. Dark-acclimated (30 min) FRRf measurements were also made on each sample prior to experimentation. All excitation and emission sequences were averaged into 1 min intervals to improve SNRs and were subsequently processed using v4 software (see Suggett et al. 2003, 2004). This routine fits the model of Kolber et al. (1998) to the excitation:emission ratio providing values of the minimum (F_o, F') and maximum (F_m, F_m') fluorescence, the effective absorption cross section (σ_{PSII}, σ_{PSII}') and the degree of excitation energy transfer between PSII reaction centres (connectivity, ρ, ρ′) under dark-adapted (unprimed) and actinic light (primed) conditions, respectively. Blanks were measured on the cell-free preparations of each sample that were obtained by gravity filtration of small volumes (<20 ml) through GF/F filters (Cullen & Davis 2003). Calculation of all fluorescence parameters accounted for instrument-specific response, scatter and baseline functions when processed.

Photosynthetic unit size and pigments. Culture aliquots of 100 to 200 ml were gravity-filtered through 47 mm GF/F filters and gently resuspended into 4 to 5 ml of the sample to pre-concentrate samples to 1.4 – 4.2 (mean 2.0) mg chl *a* l^{-1}. The filters were not permitted to run dry, to minimize damage to the cells. The concentrated samples were dark-adapted at 20°C in the chamber of an Oxygraph O_2 electrode system (Hansatech Instruments). When a consistent rate of O_2 consumption had been obtained (typically within 30 to 50 min), the rate of O_2 evolution in response to ST saturating blue LED light flashes (provided by a custom-built array of blue LEDs) was measured as described previously (Suggett et al. 2003, 2004) to estimate the photosynthetic unit (PSU) size. Briefly, this ST flash approach provides a measure of the O_2 evolved by

Table 3. Mean (±SE) values of the daily growth rate (µ, d^{-1}), maximum PSII photochemical efficiency (F_v/F_m, dimensionless), and photosynthetic unit size of PSII ($1/n_{PSII}$, mol chl *a* [mol RCII]$^{-1}$) for all species at each growth photon flux density (PFD). Clonal designations are the codes assigned by the Guillard Provasoli Center for the Culture of Marine Phytoplankton (CCMP) except for the local isolates. E/E_k is the irradiance exposure during the incubation relative to the saturating parameter from a parallel photosynthesis vs. irradiance incubation

Species	PFD	µ	F_v/F_m	$1/n_{PSII}$	E/E_k
Aureococcus anophagefferens	18	0.22 (0.02)	0.52 (0.02)	951 (13)	2.9 – 54
(CCMP1790)	80	0.40 (0.01)	0.50 (0.02)	879 (16)	0.68 – 14.9
Dunaliella tertiolecta	18	0.28 (0.03)	0.57 (0.03)	742 (11)	0.44 – 9.31
(CCMP 1320)	80	1.72 (0.05)	0.54 (0.03)	639 (18)	0.34 – 7.40
	300	2.42 (0.12)	0.54 (0.03)	501 (22)	0.06 – 2.34
Prorocentrum minimum	18	0.24 (0.01)	0.54 (0.03)	535 (10)	0.18 – 4.06
(Choptank isolate)	80	0.73 (0.06)	0.51 (0.02)	499 (9)	0.18 – 5.94
	300	1.10 (0.09)	0.46 (0.02)	448 (10)	0.09 – 2.67
Pycnococcus provasolii	18	0.31 (0.01)	0.41 (0.04)	938 (6)	0.96 – 17.0
(CCMP 1203)	80	0.73 (0.06)	0.42 (0.03)	834 (21)	0.70 – 11.8
	300	0.87 (0.02)	0.33 (0.03)	587 (24)	0.28 – 7.47
Storeatula major	18	0.27 (0.01)	0.57 (0.03)	522 (9)	0.23 – 6.16
(Choptank isolate)	80	1.01 (0.05)	0.57 (0.02)	518 (5)	0.47 – 9.12
	300	1.40 (0.06)	0.55 (0.03)	445 (16)	0.13 – 2.80
Thalassiosira weissflogii	18	0.24 (0.02)	0.56 (0.02)	584 (8)	0.18 – 3.49
(CCMP 1047)	80	1.37 (0.03)	0.53 (0.02)	520 (14)	0.14 – 5.53

functional PSII reaction centres (RCIIs). The chl *a* concentration divided by the O_2 flash yield provides the 'Emerson & Arnold number', which is termed PSU_{O2} (mol chl *a* [mol O_2]$^{-1}$). The PSU size of PSII, which is termed $1/n_{PSII}$ (mol chl *a* [mol RCII]$^{-1}$; Kolber & Falkowski 1993), is determined by dividing PSU_{O2} by 4, under the assumption that 4 electron transfer events are required for each O_2 evolved. We use the term n_{PSII} to describe the concentration of PSII reaction centres per unit of chl *a* (mol RCII [mol chl *a*]$^{-1}$).

Fluorescence-based determinations of PSII productivity. Absolute PSII electron transfer rate (ETR_{PSII}), averaged over each minute of FRRf data acquisition (mol e$^-$ [mol chl *a*]$^{-1}$ min^{-1}) was determined as follows:

$$ETR_{PSII} = E \times a_{PSII}^{*} \times \phi_{PSII} \times (6 \times 10^{-4}) \quad (2)$$

where E and ϕ_{PSII} are as in Eq. (1) and a_{PSII}^{*} is the chl *a*-specific rate of light absorption by PSII (m^2 [mol chl *a*]$^{-1}$). Inclusion of the factor 6×10^{-4} converts µmol photons to mol photons and seconds to minutes. A value for a_{PSII}^{*} was determined for each culture from the product of the dark-adapted effective absorption cross section (σ_{PSII}) and n_{PSII}, and from F_v/F_m (=(F_m–F_o)/F_m) since σ_{PSII} will be reduced relative to a_{PSII} by non-radiative loss terms to the same extent as F_v/F_m (Kolber et al. 1998, their Eq. 14):

$$a_{PSII}^{*} = \frac{[(\sigma_{PSII} \cdot n_{PSII}) \cdot 6023]}{F_v / F_m} \quad (3)$$

Values of σ_{PSII} from the FRR fluorometer are in units of Å^2 quantum^{-1}; the factor 6023 accounts for conversion of Å^2 to m^2 and quanta to mol RCII (see Suggett et al. 2006a). Values for ϕ_{PSII} were determined from measures of F', F_m', σ_{PSII}' and F_v/F_m for each ST acquisition (Suggett et al. 2006a):

$$\phi_{PSII} = F_q'/F_v' \cdot \left(\sigma_{PSII}'/\sigma_{PSII}\right) \cdot F_v/F_m \cdot \phi_{RC} \quad (4)$$

where F_q'/F_v' (= [F_m' – F']/[F_m' – F_o']) is the operating efficiency, which is also referred to as the extent of photochemical quenching or qP. For the calculation of F_q'/F_v', F_o' was not measured but estimated indirectly using fluorescence yields under actinic and initial dark-acclimated conditions (see Suggett et al. 2003): $F_o' = F_o/[(F_m - F_o)/F_m + (F_o/F_m')]$. Normalisation of σ_{PSII}' to the corresponding dark-acclimated effective absorption (σ_{PSII}) yields a measure of the reversible non-photochemical quenching component of the PSII efficiency via the antennae bed while F_v/F_m accounts for all other non-light-induced radiative losses. Finally, ϕ_{RC} (mol e$^-$ [mol photon]$^{-1}$) accounts for the quantum yield of PSII reaction centres and is assumed to be a constant of 1 mol electron transferred from the P680 complex to the primary quinone acceptor molecule per mol photon absorbed and delivered to the reaction centre (Kolber & Falkowski 1993). Substitution of Eqs. (3) & (4) into Eq. (2) gives ETR_{PSII} (mol e$^-$ [mol chl *a*]$^{-1}$ min^{-1}) as:

$$ETR_{PSII} = E \cdot n_{PSII} \cdot \sigma_{PSII}' \cdot F_q'/F_v' \cdot 3.614 \quad (5)$$

All measurements of σ_{PSII}' (σ_{PSII}) used in Eqs. (2) to (4) were spectrally adjusted to account for the weighting of light absorption by the excitation spectrum of the FRR fluorometer LEDs (peak wavelength of excitation is 478 nm). For this we extrapolated values of σ_{PSII}' measured by the FRR fluorometer across all wavelengths using PSII fluorescence excitation spectra measured between 400 and 700 nm (as in Suggett et al. 2007). Fluorescence excitation spectra were recorded from aliquots of the concentrated cultures, using a fluorescence spectrometer (Perkin-Elmer LS50B, Perkin-Elmer) with the monochromator on the detector set to 730 nm emission (Suggett et al. 2004). Samples were treated with 3-(3,4-dichlorophenyl)-1,1-dimethylurea (DCMU) and pre-illuminated to close all PSII reaction centres. The fluorescence excitation at each wavelength is termed F_{730} (λ). Thus, spectrally resolved values of the effective absorption, σ_{PSII}' (λ), were determined as:

$$\sigma_{PSII}'(\lambda) = \left(\sigma_{PSII}'(478)/F_{730}(478)\right) \cdot F_{730}(\lambda) \quad (6)$$

All FRRf-determined values of σ_{PSII}' (σ_{PSII}) were then spectrally adjusted for the actinic light source as:

$$\overline{\sigma_{PSII}'} = \left(\sum_{400}^{700} \sigma_{PSII}'(\lambda) \cdot E(\lambda)\right) \Delta\lambda \Big/ \sum_{400}^{700} E(\lambda)\,\Delta\lambda \quad (7)$$

where E(λ) is the spectrally resolved light intensity for the actinic light source, which was determined using a USB2000 spectroradiometer (Ocean Optics) and converted from energy-based to quantum-based units (Kirk 1994). Rearrangement of Eqs. (5) & (7) yields the final equation used to determine ETR_{PSII} (mol e$^-$ [mol chl *a*]$^{-1}$ min^{-1}) for each minute of FRRf data acquisition (see Fig. 1):

$$ETR_{PSII} = E \cdot n_{PSII} \cdot \overline{\sigma_{PSII}'} \cdot F_q'/F_v' \cdot 3.614 \quad (8)$$

Values of F_q'/F_v' and σ_{PSII}' were not constant throughout the period of isotope incubation (Fig. 1). For comparison within and between methods, all values of ETR were integrated over the duration of the incubation and standardised to an hourly integrated rate, ETR_{PSII}, in mol e$^-$ [mol chl a^{-1}] h^{-1}:

$$ETR_{PSII} = \left(\sum_{t(start)}^{t(end)} ETR_{PSII}(t)\,\Delta t\right) \cdot \left(60/\sum t\right) \quad (9)$$

where t is time (min) and 60 is a factor to convert minutes to hours.

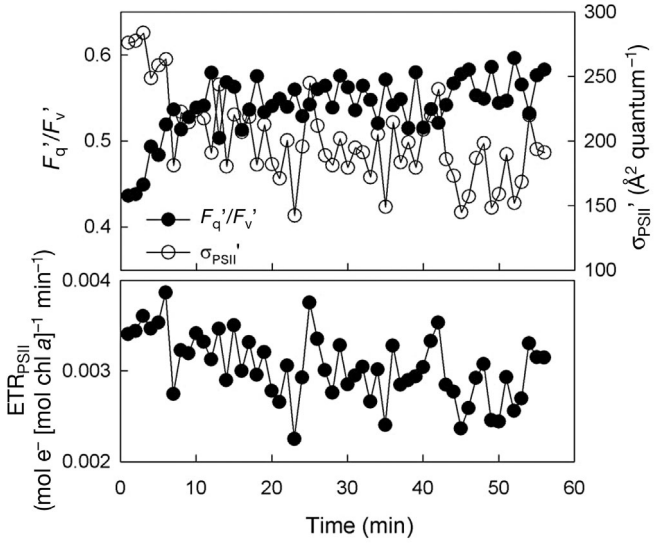

Fig. 1. Variation in fast repetition rate (FRR) fluorescence-based variables during a single gas-exchange incubation experiment (example shown is for low-light grown *Dunaliella tertiolecta*). Values for the minimum and maximum fluorescence yield (F' and F_m', respectively) and the PSII effective absorption (σ_{PSII}', Å^2 quantum^{-1}) were obtained by integrating all FRR fluorescence transients obtained at 1 min intervals (~160 acquisitions) to increase the signal to noise ratio. Values for the PSII operating efficiency (F_q'/F_v', dimensionless) were determined from F_m' and F' relative to the corresponding dark-acclimated measurements made prior to experimentation. The electron transfer rate (ETR$_{PSII}$) was calculated for each 1 min interval (Eq. 8) and integrated to yield an hourly rate (Eq. 9). See text for details

O_2 exchange, C uptake and chl *a* concentration. A modified ^{18}O isotope dilution technique for discrete samples (Kana 1990) was used to measure gross uptake and gross evolution of O_2 in the light. Net photosynthesis was calculated by difference. A sample of culture was drawn into a 100 ml syringe after being partially degassed by sparging with nitrogen (N_2). A bubble of $^{18}O_2$ was then introduced and partially equilibrated with the sample by gentle rocking. Four 7 ml glass tubes were filled to overflowing and sealed with glass stoppers. The initial concentrations of $^{18}O_2$ (mass 36) and $^{16}O_2$ (mass 32) were determined from 2 of the tubes. The remaining 2 tubes were incubated in front of the detection window of the FRR fluorometer. After the appropriate incubation period, the samples were immediately analyzed for $^{18}O_2$ and $^{16}O_2$. Analysis time per sample was typically ~2 min. The dissolved O_2 isotope measurements were done using a membrane inlet mass spectrometer (Bay Instruments), which provides dissolved isotope concentration data as well as ratios and differs from the original technique (Kana 1990). Chl *a*-normalised rates of O_2 uptake and evolution (mol O_2 [mol chl a]$^{-1}$ h^{-1}) were calculated using isotopic dilution equations (Kana 1990).

Carbon uptake was calculated in an analogous fashion. Two of the gas-tight tubes were filled with sample that had been spiked with $NaH^{14}CO_3$ (17441H from MP Biomedicals) at a concentration of ~1 µCi ml^{-1} and were incubated over the detection window of the FRR fluorometer. The initial concentration of ^{14}C was determined from subsamples transferred into a scintillation cocktail containing 50 µl ml^{-1} of β-phenylethylamine. At the end of the incubation, 3 × 1 ml subsamples from each of the spiked tubes were pipetted into scintillation vials containing 50 µl of formalin. These were acidified with 250 µl of 6N HCl and shaken for an hour to remove residual inorganic carbon, before adding the scintillation cocktail and counting. Carbon uptake (mol CO_2 [mol chl a]$^{-1}$ h^{-1}) was calculated from the concentration of total dissolved inorganic carbon and the proportion of the ^{14}C tracer that was fixed during the incubation, after normalization to the duration of the incubation and chlorophyll concentration. An isotopic discrimination factor of 1.06 was used. The concentration of dissolved inorganic carbon (DIC) was determined using a Shimadzu total organic carbon (TOC) analyzer (Shimadzu Scientific Instruments).

Post-hoc testing using paired *t*-test showed that there was no significant difference ($p > 0.05$) in estimates of gross O_2 evolution or O_2 uptake between the 2 tubes spiked with $^{18}O_2$ across all experiments. In contrast, there was a significant difference ($p < 0.001$) between the 2 tubes spiked with $NaH^{14}CO_3$, such that values of carbon fixation were consistently lower for the upper tube (i.e. the highest tube in the array) than for the lower tube (which was between the 2 tubes enriched with $^{18}O_2$). These lower values were attributed to a fall-off in light intensity towards the top of the stack of tubes; thus, the data from the uppermost tube was discarded. Measurements of O_2 flux for each replicate experiment are therefore averages of paired samples while those of carbon fixation are from a single sample.

All productivity measurements were normalised to the chlorophyll concentration. Aliquots of each sample culture used for experimentation were collected on Whatman GF/F filters, frozen in liquid nitrogen, and held at −80°C for later quantification of chl *a* by high pressure liquid chromatography (Van Heukelem et al. 1992).

RESULTS

Cell growth, potential photochemical efficiency and PSU size of PSII

All species exhibited growth rates that were similar (~0.25 d^{-1}) at the lowest growth PFD but more variable at the mid to high growth PFDs (Table 3). The highest

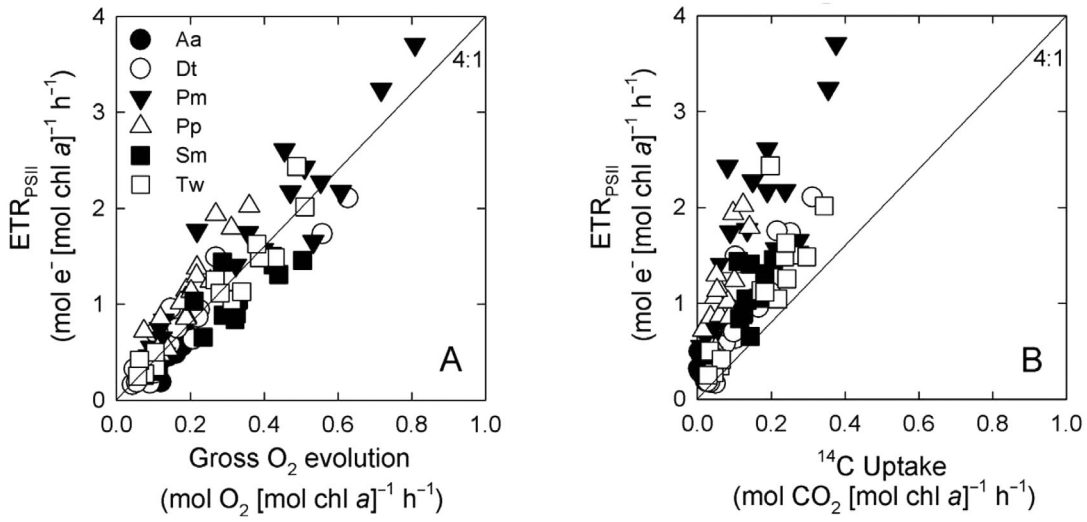

Fig. 2. Comparative measurements of photosynthesis using alternative 'currencies' for all phytoplankton species examined. Aa: *Aureococcus anophagefferens*; Dt: *Dunaliella tertiolecta*; Pm: *Prorocentrum minimum*; Pp: *Pycnococcus provasolii*; Sm: *Storeatula major*; Tw: *Thalassiosira weissflogii*. Fast repetition rate fluorometry-based electron transfer rate (ETR) vs. (A) mass inlet membrane spectrometer (MIMS)-based gross O_2, and (B) ^{14}C uptake. The ratio between ETR and gross O_2 production is the quantum requirement for O_2 evolution by PSII, ϕ_e; solid line represents a 4:1 ratio between currencies. Corresponding regression coefficients are given in Tables 3 & 5. In the case of (A), the solid line can also represent a 1:1 line if the ETR is multiplied by ϕ_e that is set to the assumed constant minimum value of 4 mol O_2 [mol e$^-$]$^{-1}$

growth rates were observed for *Dunaliella tertiolecta*. Dark-acclimated measurements of the maximum PSII photochemical efficiency (F_v/F_m, dimensionless) and PSU size ($1/n_{PSII}$, mol chl *a* [mol RCII]$^{-1}$), were made prior to experimentation (Table 3). Measures of F_v/F_m from cells grown under low irradiance were highest for *D. tertiolecta* and *Storeatula major* (0.57) and lowest for *Pycnococcus provasolii* (0.41). As expected, values of F_v/F_m decreased with increasing growth PFD. The decrease was ~10% for all species, except for *P. provasolii* which declined by 25%. Estimates of $1/n_{PSII}$ under low-light growth were lowest for *Prorocentrum minimum* and *S. major* and highest for *Aureococcus anophagefferens* and *P. provasolii*, although all decreased with increasing growth PFD. Values of $1/n_{PSII}$ decreased by ~20 to 25% for all species, except for *P. provasolii* which decreased by ~40 to 50%.

Comparing ETRs with gross O_2 evolution

The ETR_{PSII} calculated from FRR fluorescence was linearly related to the rate of gross O_2 evolution in all species examined (Fig. 2A, Table 4). The slope of this

Table 4. Summary results of Bartlett's type II model regressions showing the slope (±SE) and coefficient of determination (adjusted r^2) for comparisons of the fast repetition rate fluorometry-based ETR_{PSII} (mol e$^-$ [mol chl *a*]$^{-1}$ h^{-1}) with mass inlet membrane spectrometer (MIMS)-based gross O_2 production (mol O_2 [mol chl *a*]$^{-1}$ h^{-1}); and ^{14}C-based carbon uptake (mol CO_2 [mol chl *a*]$^{-1}$ h^{-1}). The slope represents the relationship between alternative photosynthetic currencies across all growth and exposure photon flux densities, and hence represents a mean 'exchange rate'. Values are given for analyses from each individual species and from all data combined. All values of r^2 are significant ($p < 0.05$), except where indicated (NS, not significant)

Species	ETR_{PSII} (*y*) vs. gross O_2 (*x*) (mol e$^-$ [mol O_2]$^{-1}$)		ETR_{PSII} (*y*) vs. CO_2 (*x*) (mol e$^-$ [mol CO_2]$^{-1}$)		
	r^2	slope	r^2	slope	intercept
Aureococcus anophagefferens	0.64	3.71 (0.19)	NS	3.63 (3.59)	0.34 (0.20)
Dunaliella tertiolecta	0.77	3.63 (0.23)	0.84	6.63 (0.71)	0.09 (0.09)
Prorocentrum minimum	0.81	4.32 (0.19)	0.69	7.27 (1.18)	0.64 (0.21)
Pycnococcus provasolii	0.79	5.66 (0.22)	0.59	11.55 (2.29)	0.28 (0.17)
Storeatula major	0.75	3.40 (0.17)	0.77	5.99 (0.79)	0.20 (0.15)
Thalasiosira weissfloggii	0.85	3.98 (0.15)	0.69	5.37 (0.95)	0.18 (0.19)
All data combined	0.81	4.12 (0.11)	0.61	6.26 (0.50)	0.35 (0.07)

relationship varied significantly among species (Table 4), with values ranging from 15% below to 40% above the expected value of 4 mol e^- [mol O_2]$^{-1}$. Specifically, values for ϕ_e ranged from 3.4 (*Storeatula major*) to 5.6 (*Pycnococcus provasolii*) (Table 4, but see Table 5 for ANCOVA post-hoc groupings).

All comparisons were performed using Bartlett's type II linear regressions. Two important considerations must be taken into account when evaluating the results obtained with this approach. Firstly, the intercept was initially maintained as a free-fitting parameter; however, the intercept term (coefficient ± SE) was found not to be significantly different from 0 (*t*-test, $p < 0.05$, not shown) in all cases. Thus, we chose to recalculate these regressions by setting the intercept to 0, i.e. we required that there can be no O_2 evolution in the absence of electron transport and vice versa. This procedure is important since the exchange rate between currencies equals the regression slope only when the intercept is 0. Secondly, using a linear regression assumes that the slope of the relationship between ETR_{PSII} and gross O_2 evolution, i.e. ETR_{PSII}/gross O_2 evolution (= ϕ_e), is constant and therefore independent of light intensity. Although there is evidence that ϕ_e may be reduced under extremely high (Prášil et al. 1996) or low (Quigg et al. 2006) light intensities, we did not observe significant non-linearity over the range of actinic PFDs used in our experiments.

Comparing ETRs with $^{14}CO_2$ fixation

The ETR_{PSII} was linearly related to $^{14}CO_2$ fixation, although both the slopes and the intercepts varied substantially among the species examined (Fig. 2B). Significant linear correlations were found for 5 of the 6 species examined (Table 4). The exception was *Aureococcus anophagefferens*, for which the range of irradiance was higher relative to E_k than for the other species (Table 3). Unlike the comparison of ETR_{PSII} with gross O_2 evolution in which we fixed the intercept to 0, we allowed the intercept to be a free parameter for the linear regression of ETR_{PSII} against $^{14}CO_2$ fixation rate. This is because processes associated with low light (e.g. overestimation of net CO_2 uptake by ^{14}C fixation; Johnson & Barber 2003) or high light (e.g. underestimation of net and gross CO_2 uptake by ^{14}C fixation due to alternative oxidase cycling of newly fixed carbon; Raghavendra & Padmasree 2003) may alter the slope. Without constraining the regression fit to the origin, data for *Pycnococcus provasolii* and *Prorocentrum minimum* yielded an intercept that was >0; in contrast, all other species yielded an intercept that was not significantly different from 0 (*t*-test, $p < 0.05$, not shown).

As expected, the values for mol e^- [mol CO_2]$^{-1}$ were greater than those observed when comparing the ETR_{PSII} and gross O_2 production (Tables 4 & 5). Furthermore, the range of values for the ETR_{PSII}:C uptake ratio across all taxa (3.6 to 11.6, i.e. 3.2-fold; or 5.4 to 11.6, i.e. 2.1-fold, if we exclude the non-significant result for *Aureococcus anophagefferens*) was also greater than that for the ETR_{PSII}:O_2 evolution ratio (3.6 to 5.7, i.e. 1.6-fold). Pooled data from all species yielded a value of 6.3 ± 0.35 mol e^- [mol CO_2]$^{-1}$; however, species-specific values ranged from ~4 to 12 (Table 4). The ANCOVA and post-hoc Tukey's test (Table 5) yielded 3 distinct groups (excluding *A. anophagefferens*) for both the slope and the intercept: *Dunaliella tertiolecta*, *Storeatula major* and *Thalassiosira weissflogii* (slope of ~5.4 to 6.6 and intercept not significantly different from 0); *Prorocentrum minimum* (slope of ~7.3 and intercept of ~0.6); and *Pycnococcus provasolii* (slope of ~12 and intercept of ~0.3) (Fig. 2).

Table 5. Tukey's test post-hoc analysis of covariance (ANCOVA) groupings performed to test for significant differences between regression slopes comparing different photosynthetic currencies (Table 4). Also shown is the post-hoc test for intercepts of comparisons of ETR_{PSII} and CO_2, and gross and net O_2 evolution (Table 4). Species (Aa, *Aureococcus anophagefferens*; Dt, *Dunaliella tertiolecta*; Pm, *Prorocentrum minimum*; Pp, *Pycnococcus provasolii*; Sm, *Storeatula major*; Tw, *Thalassiosira weissflogii*) that were not significantly different from one another are grouped within square brackets; each set of square brackets indicates significantly different groups of species while hyphens indicate overlapping groupings

Photosynthetic currency	Post-hoc test groupings
Regression slope comparison	
ETR_{PSII} (*y*) vs. MIMS gross O_2 (*x*)	[Sm]-[Aa, Dt]-[Tw]-[Pm], [Pp]
ETR_{PSII} (*y*) vs. C (*x*)	[Aa]-[Dt, Sm, Tw]-[Pm], [Pp]
Gross O_2 (*y*) vs. Net O_2 (*x*)	[Aa], [Dt]-[Tw]-[Sm, Pm, Pp]
Net O_2 (*y*) vs. C (*x*)	[Pm, Tw]-[Pp]-[Sm, Dt], [Aa]
Intercept comparison	
ETR_{PSII} (*y*) vs. C (*x*)	[Dt, Tw, Sm]-[Pp, Aa], Pm
Gross O_2 (*y*) vs. Net O_2 (*x*)	[Aa, Dt, Pp, Sm, Tw], [Pm]

Comparing net with gross O_2 evolution and $^{14}CO_2$ uptake

Rates of net O_2 evolution were compared with gross O_2 evolution and C uptake (Fig. 3A, Table 6). In comparing gross and net O_2 evolution, the slope reflects the average light enhancement of respiration and the intercept is the dark respiration rate. This analysis ignores the different irradiance dependencies of gross evolution and uptake in microalgae (Kana

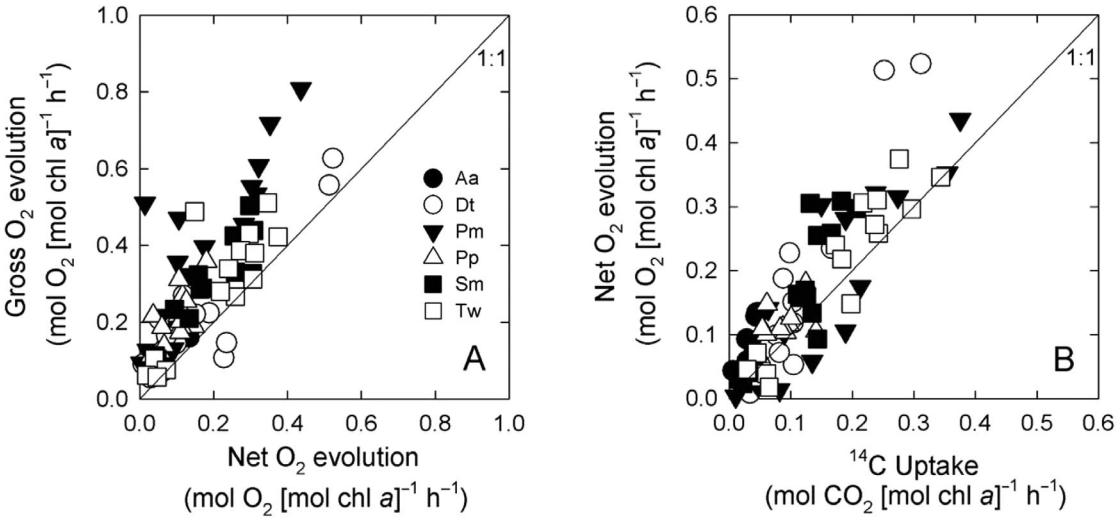

Fig. 3. Comparative measurements of photosynthesis using alternative 'currencies' for all phytoplankton species examined. (A) Mass inlet membrane spectrometer (MIMS)-based gross O_2 vs. MIMS-based net O_2 and (B) MIMS-based net O_2 vs. ^{14}C uptake. The differences between gross and net O_2 and between net O_2 and CO_2 uptake are the proportion of gross O_2 consumed in the light and the photosynthetic quotient, respectively. The solid line indicates a 1:1 ratio; symbol abbreviations are as in Fig. 2. Corresponding regression coefficients are given in Table 6

1992, Lewitus & Kana 1995). Pooled data from all species yielded a slope of gross vs. net O_2 evolution of 1.12 ± 0.08 mol O_2 [mol O_2]$^{-1}$. Thus, the light-driven enhancement of respiration accounted for ~12% of the gross photosynthesis. Again, substantial variability was observed between species (Tables 5 & 6): values were highest for *Storeatula major*, *Prorocentrum minimum* and *Pycnococcus provasolii* (1.2 to 1.3), while values were not significantly different from 1 (i.e. no light-dependent enhancement of O_2 consumption) for *Dunaliella tertiolecta* and *Thalassiosira weissflogii*. Intercept values for the gross:net O_2 evolution ratio were the same for all species (~0.07 to 0.08 mol O_2 [mol O_2]$^{-1}$), except for *P. minimum* for which the value was approximately 2× as high (~0.17).

Simultaneous estimates of net O_2 evolution and CO_2 uptake were compared to generate values for the 'conventional' photosynthetic quotient (PQ) (Fig. 3B). Pooled data from all species yielded a slope with a value of 1.24 ± 0.05 mol O_2 [mol CO_2]$^{-1}$ (Table 6). Values of the PQ were lowest (~1.1) for *Thalassiosira weissflogii* and *Prorocentrum minimum*, and highest (~1.6) for *Dunaliella tertiolecta* (Table 6). The very high value for *Aureococcus anophagefferens* (~2.5, Table 6)

Table 6. Summary results of Bartlett's type II model regressions showing the slope (±SE) and coefficient of determination (adjusted r^2) for comparisons of mass inlet membrane spectrometer (MIMS)-based gross and net O_2 production (mol O_2 [mol chl a]$^{-1}$ h^{-1}) and MIMS-based net O_2 production (mol O_2 [mol chl a]$^{-1}$ h^{-1}) and ^{14}C-based carbon uptake (mol CO_2 [mol chl a]$^{-1}$ h^{-1}). The slope represents the relationship between alternative photosynthetic currencies across all growth and exposure photon flux densities, and hence represents a mean 'exchange rate'. All values of r^2 are significant ($p < 0.05$), except where indicated (NS, not significant). In comparing gross and net O_2 evolution, the slope and the intercept reflect the proportion of gross O_2 consumed in the light and dark, respectively. Note that some values of calculated net O_2 evolution for *Aureococcus anophagefferens* were negative and have not been included in these analyses

Species	Gross O_2 (y) vs. net O_2 (x) (mol O_2 [mol O_2]$^{-1}$)			Net O_2 (y) vs. CO_2 (x) (mol O_2 [mol CO_2]$^{-1}$)	
	r^2	slope	intercept	r^2	slope
Aureococcus anophagefferens	NS	0.74 (0.24)	0.07 (0.02)	NS	2.50 (0.39)
Dunaliella tertiolecta	0.81	0.91 (0.12)	0.07 (0.03)	0.76	1.61 (0.14)
Prorocentrum minimum	0.73	1.31 (0.20)	0.17 (0.04)	0.70	1.09 (0.10)
Pycnococcus provasolii	0.59	1.26 (0.25)	0.08 (0.02)	0.53	1.23 (0.09)
Storeatula major	0.70	1.22 (0.11)	0.07 (0.02)	0.74	1.46 (0.07)
Thalassiosira weissfloggii	0.70	1.04 (0.16)	0.08 (0.04)	0.82	1.13 (0.06)
All data combined	0.68	1.12 (0.08)	0.10 (0.02)	0.76	1.24 (0.05)

was based on a regression that was not statistically significant ($p > 0.05$). Values for the other species were 1.2 to 1.6 mol O_2 [mol CO_2]$^{-1}$.

DISCUSSION

Prior comparisons of ETR_{PSII} with O_2 evolution and/or CO_2 uptake have employed different incubation conditions for the alternate photosynthetic currencies that were measured. This adds uncertainty in attempts to compare ETR_{PSII} with gas exchange rates because differences in the rates may have arisen as a result of differences in the duration of the experiments, confinement artifacts, and variability in the intensity or spectral quality of the actinic light. A further difficulty in comparing ETR_{PSII} with gas exchange rates is that the SNR decreases for FRRf but increases for gas exchange measurements as actinic light intensity increases. Because ETR_{PSII} scales directly with light intensity, errors in calculating ETR_{PSII} will be proportional to errors in measuring light intensity. Such errors certainly introduce variability in data collected under low and high light, where intensity is expressed relative to the saturating parameter for photosynthesis, E_k. Our measurements minimised these issues since ETR_{PSII} and gas exchange rates were measured on the same samples (thus under identical conditions) and the comparisons were made at moderate ranges of E/E_k. Nonetheless, variation in the exchange rates among ETR_{PSII}, gross O_2 evolution and ^{14}C fixation are evident.

Does FRRf yield gross O_2 production?

The question of how well the FRRf estimate of linear electron transfer approximates gross O_2 evolution is of primary importance to the application of the fluorescence approach to productivity studies. To date, most studies using FRRf have assumed a quantum yield of electron transfer (ϕ_e) with a value of 4 mol e^- [mol O_2]$^{-1}$ to scale the ETR_{PSII} to gross O_2 productivity, since a theoretical minimum of 4 electron transfers is required to evolve 1 molecule of O_2 from the water oxidizing complex of PSII. Importantly, our ETR_{PSII} determinations contain a measure of n_{PSII}, which inherently accounts for ϕ_e that equal a value of 4 mol e^- [mol O_2]$^{-1}$ (see 'Materials and methods', also Suggett et al. 2006a). On average, the comparison of ETR_{PSII} and gross O_2 evolved did not deviate significantly from a value of 4 (Table 4), thus indicating that FRRf indeed provides a robust estimate of ETR_{PSII} and ultimately gross O_2 evolved (at least for the taxa and environmental conditions investigated here). However, some species clearly appear to complicate this general observation.

Our estimated values of ϕ_e were significantly higher and lower than 4 mol e^- [mol O_2]$^{-1}$ for *Pycnococcus provasolii* and *Storeatula major*, respectively (Tables 4 & 5). Values of $\phi_e < 4$ are difficult to reconcile on biochemical and bioenergetic grounds and we need to consider sources of error that may lead to an overestimation of gross O_2 flux and/or underestimation of ETR_{PSII}. In terms of undetected calibration problems with the mass spectrometry, we note that any intracellular isotope cycling that would not be detected by our measurement technique would, in fact, lead to an underestimate of gross O_2 uptake and evolution rather than an explanatory overestimate. If we accept that gross O_2 evolution rates were not systematically overestimated, then values of $\phi_e < 4$ most likely resulted from an underestimation of the rate of light absorption by PSII. Errors could enter such a calculation due to inaccuracy in measuring (1) the photon flux density and/or spectral quality of the actinic light source, (2) the alteration in light quality and/or quantity by the geometric properties of the incubation vessels, and hence in light incident upon the phytoplankton cells, (3) the absolute value and spectral dependence of the effective cross section of photosystem II, and (4) the concentration of functional PSII reaction centres in the sample. Although errors (1) & (2) would apply to all species examined, their magnitude will depend on the convolution of the spectrum of the actinic light source with that of the effective cross section of PSII. Errors (3) & (4) are expected to vary due to the pigment complement and molecular organization of the light harvesting apparatus. Error (3) could also arise through inaccurate calibration of the FFRf's excitation source.

For values of $\phi_e > 4$, we note that 2 mechanisms have been proposed to decouple linear ETR from gross O_2 evolution at the reaction centres. First, cyclic flow around PSII may occur at very high light (Prášil et al. 1996). Second, electron 'slippage' may occur at very low light (Quigg et al. 2006). Cyclic flow describes rerouting of electrons via cytochrome *b* from reduced primary acceptor quinone molecules (Q_A) back to the core chl *a* molecule in the PSII reaction centre once the plastoquinone pool becomes reduced. Electron 'slippage' refers to the decay of unstable intermediate S states of the PSII reaction centres with primary and secondary quinone acceptor molecule (Q_A/Q_B) charge recombination during the process of water splitting. Both mechanisms are light dependent. To date, these mechanisms have only been investigated for chlorophytes and diatoms (Prášil et al. 1996, Feikema et al. 2006, Quigg et al. 2006). However, we did not observe any light dependency of ϕ_e, or values that were significantly different from 4 mol e^- [mol O_2]$^{-1}$, for the chlorophyte and diatom tested here. This is perhaps not surprising, since cyclic electron flow around PSII and slippage op-

erate at light intensities outside the range of test irradiances used here (Table 3).

Reductant flow, O_2 consuming pathways and PQ

One of the causes of an elevated ETR requirement for CO_2 assimilation is the diversion of photosynthetic reductant to pathways that reduce other compounds. Besides CO_2, reduction of nitrite (NO_2^-) and sulfate (SO_4^{-2}) occurs in chloroplasts during photosynthesis as part of normal nitrogen (N) and sulfur (S) assimilatory pathways. We would expect the reductant demand for N and S assimilation to be ~25% of the total reductant flux for cells here grown on nitrate (NO_3^-) and SO_4^{-2} (based on the elemental ratios of phytoplankton biomass and the reductant requirements for C, N, and S assimilation); consequently, the ETR:CO_2 ratio which ranged from 5.4 (*T. weissfloggii*) to 11.6 (*Pycnococcus provasolii*) (Table 4) was expected. The ratio for *Aureococcus anophagefferens* was anomalously low at 3.6, but the relationship was not statistically significant. The lack of significant relationships among all currencies for this species (Tables 4 & 6) may be related to the high relative irradiance, expressed as E/E_k, for this species (Table 3).

For most species examined here, a significant amount of reductant was directed to one or more additional acceptors (beyond C, N, and S reduction) based on the extent to which the ETR:CO_2 ratio exceeded the reference value of 5. Oxygen is clearly an acceptor in those cases where the slope of gross O_2 vs. net O_2 fluxes exceeded a value of 1 (Table 6). A slope of 1 would be obtained if O_2 uptake (respiration) were constant (i.e. independent of irradiance). A slope <1 would indicate a decline in O_2 uptake with increasing irradiance and a slope >1 would indicate an increase in O_2 uptake with increasing irradiance. Only 3 of the species (*Prorocentrum minimum*, *Pycnococcus provasolii* and *Storeatula major*) had slopes that were 20 to 30% >1, indicating light-stimulated O_2 uptake, which is consistent with other species from the same taxonomic groups (25 to 35%: Lewitus & Kana 1995, Eriksen & Lewitus 1999; 35 to 50%: Suggett et al. 2008). Curiously, we did not observe any light-stimulated O_2 uptake for *Thalassiosira weissfloggi* and *Dunaliella tertiolecta*, as might have been expected given previous studies of green algae and diatoms (Weger et al. 1988, 1989, Luz et al. 2002).

Although this analysis of linear slopes is convenient for assessing broad patterns in O_2 cycling and potentially useful in ecological applications, the light-dependency of O_2 uptake is more complex and potentially nonlinear. Lewitus & Kana (1995) provided a conceptual model of the effect of light on O_2 uptake, noting the potential activity of the Mehler reaction, chlororespiration, 'normal' mitochondrial respiration and alternative respiration. To this we can add the potential for photorespiration, although little is known about its relationship to light in algae. The potential for oxygenase activity by rubisco is thought to be less than that for other O_2 consuming pathways in algae (Badger et al. 2000). Differences in the structure of rubisco between chromophytic algae and the vascular plant lineage also lead to a higher specificity for CO_2 over O_2 in the chromophytes, and a reduced likelihood of oxygenase activity (Zhu et al. 1998).

In principle, a slope <1 for gross vs. net O_2 flux could be the result of chlororespiratory shutdown, although this is probably not relevant here: the chlororespiration that occurs in darkness is shut down under very low light intensities, which are sufficient to open up the reductant pathway to PSI. Generally, however, the effect of light on O_2 uptake over the range from dim irradiance to saturating irradiance for photosynthesis may range from close to nil to highly stimulatory, particularly at light-saturated photosynthesis. Indeed, it is common to observe O_2 uptake rates as high as 30 to 40% of the gross O_2 evolution rate in cultivated algae under saturating light (Weger et al. 1988, 1989, Lewitus & Kana 1995, Eriksen & Lewitus 1999, Suggett et al. 2008), which means that 30 to 40% of photosynthetic reductant is directed to O_2 reduction rather than to anabolism.

Much remains to be learned regarding the degree to which this high rate of O_2 cycling is linked to energy dissipation or ATP synthesis by pseudocyclic photophosphorylation. The Mehler reaction is presumably tied to photophosphorylation because O_2 reduction occurs downstream of PSI. Recently, chlororespiratory activity has been ascribed to a plastid terminal oxidase (PTOX) that is associated with intersystem components of the photosynthetic electron transport chain between PSII and PSI (e.g. Behrenfeld et al. 2004, Bailey et al. 2008, Cardol et al. 2008, Mackey et al. 2008). There is some indication that PTOX may be active in the light and that it receives electrons from plastoquinol, which would circumvent the translocation of protons across the thylakoids. As such, it would serve as an energy 'valve' that dissipates photosynthetic reductant energy. Such a process would potentially enable reaction centres to remain open when CO_2 fixation is saturated, thus preventing donor-side inhibition (Mackey et al. 2008).

CONCLUSIONS

This productivity comparison exercise presented here has produced a series of 'exchange rates' (factors) that interconvert between several key primary photo-

synthetic currencies (e^-, O_2, CO_2) for representatives of key phytoplankton taxa. Data collected under controlled laboratory conditions provide an objective basis for assumptions or constants that must be applied to calculate ETR_{PSII} or convert between ETRs and rates of O_2 evolution or CO_2 uptake. However, we caution that it is unlikely that currency rates for native phytoplankton assemblages will be so highly constrained because of the complexity of reductant flow in microalgae. In purely phototrophic phytoplankton, the source of energy 'starts' with PSII activity; however, the fate of that photosynthetically trapped energy (nominally reduced quinols) is manifold as it ultimately drives the reduction of all oxidized nutrients (C, N, S, etc.) and participates in energy dissipating reactions that protect the cell from excessive energy. It is particularly problematic under high irradiance regimes, such as at the ocean surface, where dissipatory processes become increasingly important.

In resolving this currency issue, we need to improve both methodology and our understanding of energy flow pathways and their regulation (see also Wagner et al. 2006). It is not trivial to obtain all of the measures needed to assess the relationship between methodologies and it is unlikely that such effort could be made in the field on a routine basis. Thus, it is likely that a multivariate approach will ultimately be required to resolve the compounding effects of environment and taxonomy on the parameterization of exchange rates between alternative photosynthetic currencies. The comparison performed here (based on linear regressions) under controlled conditions provides a very useful means with which to interpret existing field data relating ETR_{PSII} to C fixation (Table 2), since these field data span a wide range of environmental conditions and yet have been exclusively examined using linear regression.

The use of both active fluorescence and O_2 isotopic discrimination *in situ* to estimate primary productivity is increasing, and will likely continue to increase in popularity as constraints associated with measuring actual carbon fixation grow, and as researchers strive to examine productivity across larger temporal and spatial scales. Describing how both the growth environment and the phytoplankton community composition modulate the conversion of linear electron flow (and gross O_2 production) into fixed carbon is likely to remain a key priority for future studies of productivity.

Acknowledgements. The authors thank 3 anonymous reviewers for invaluable comments that improved an earlier version of this manuscript. This work was originally supported by the UK Natural Environmental Research Council (Grant NER/A/S/2000/01237 to R.J.G.) and the US National Science Foundation (NSF grant OCE-9907702 to T.M.K. and H.L.M.). We also thank the Batsheva de Rothschild Foundation, Bar Ilan University, the Moshe Shilo Center for Marine Biogeochemistry, and the staff of the Interuniversity Institute for logistic support and the EUR-OCEANS Network of Excellence for funding support. This work was presented during the 8th International Workshop of the Group for Aquatic Primary Productivity (GAP), and the Batsheva de Rothschild Seminar on Gross and Net Primary Productivity (Interuniversity Institute for Marine Sciences, Eilat, Israel, April 2008). This is contribution number 4296 of the University of Maryland Center for Environmental Science.

LITERATURE CITED

Babin M, Morel A, Falkowski PG, Claustre H, Bricaud A, Kobler ZS (1996) Nutrient- and light-dependent variations of the maximum quantum yield of carbon fixation in eutrophic, mesotrophic and oligotrophic systems. Deep-Sea Res 43:1241–1272

Badger MR, von Caemmerer S, Ruuska S, Nakano H (2000) Electron flow to oxygen in higher plants and algae: rates and control of direct photoreduction (Mehler reaction) and rubisco oxygenase. Philos Trans R Soc Lond B 355: 1433–1446

Bailey S, Melis A, Mackey KRM, Cardol P and others (2008) Alternative photosynthetic electron flow to oxygen in marine *Synechococcus.* Biochim Biophys Acta 1777: 269–276

Beardall J, Quigg AS, Raven JA (2003) Oxygen consumption: photorespiration and chlororespiration. In: Larkum A, Raven JA, Douglas S (eds) Photosynthesis in algae. Advances in photosynthesis and respiration. Kluwer, Dordrecht, p 157–181

Beer S, Vilenkin B, Weil A, Veste M, Susel L, Eshel A (1998) Measuring photosynthetic rates in seagrasses by pulse amplitude modulated (PAM) fluorometry. Mar Ecol Prog Ser 174: 293–300

Behrenfeld MJ, Prasil O, Babin M, Bruynat F (2004) In search of a physiological basis for covariation in light-limited and light-saturated photosynthesis. J Phycol 40:4–25

Behrenfeld MJ, Halsey KH, Milligan AJ (2008) Evolved physiological responses of phytoplankton to their integrated growth environment. Philos Trans R Soc Lond B 363: 2687–2703

Bender M, Grande K, Johnson K, Marra J and others (1987) A comparison of four methods for determining planktonic community production. Limnol Oceanogr 32:1085–1098

Boyd PW, Aiken J, Kolber ZS (1997) Comparison of radiocarbon and fluorescence based (pump and probe) measurements of phytoplankton photosynthetic characteristics in the Northeast Atlantic Ocean. Mar Ecol Prog Ser 149: 215–226

Cardol P, Bailleul B, Rappaport F, Derelle E and others (2008) An original adaptation of photosynthesis in the marine green alga *Ostreococcus.* Proc Natl Acad Sci USA 105: 7881–7886

Corno G, Letelier RM, Abbott MR, Karl DM (2006) Assessing primary production variability in the North Pacific subtropical gyre: a comparison of fast repetition rate fluorometry and ^{14}C measurements. J Phycol 42:51–60

Cullen JJ, Davis RF (2003) The blank can make a big difference in oceanographic measurements. Limnol Oceanogr Bull 12:29–35

Eriksen NT, Lewitus AJ (1999) Cyanide-resistant respiration in diverse marine phytoplankton: evidence for the widespread occurrence of the alternative oxidase. Aquat Microb Ecol 17:145–152

Estévez-Blanco P, Cermeño P, Espiñeira M, Fernández E (2006) Phytoplankton photosynthetic efficiency and primary production rates estimated from fast repetition rate fluorometry at coastal embayments affected by upwelling (Rías Baixas, NW of Spain). J Plankton Res 28:1153–1165

Falkowski PG, Wyman K, Ley AC, Mauzerall DC (1986) Relationship of steady state photosynthesis to fluorescence in eukaryotic algae. Biochim Biophys Acta 849:183–192

Feikema WO, Marosvölgyi MA, Lavaud J, van Gorkom HJ (2006) Cyclic electron transfer in photosystem II in the marine diatom *Phaeodactylum tricornutum.* Biochim Biophys Acta 1757:829–834

Flameling IA, Kromkamp JC (1998) Light dependence of quantum yields for PSII charge separation and oxygen evolution in eukaryotic algae. Limnol Oceanogr 43: 284–297

Franklin LA, Badger MR (2001) A comparison of photosynthetic electron transfer rates in macroalgae measured by pulse amplitude modulated chlorophyll fluorometry and mass spectrometry. J Phycol 37:756–767

Fujiki T, Suzue T, Kimono H, Saino T (2007) Photosynthetic electron transport in *Dunaliella tertiolecta* (Chlorophyceae) measured by fast repetition rate fluorometry: relation to carbon assimilation. J Plankton Res 29:199–208

Genty B, Briantais JM, Baker NR (1989) The relationship between quantum yield of photosynthetic electron transport and quenching of chlorophyll fluorescence. Biochim Biophys Acta 990:87–92

Guillard RRL (1975) Culture of phytoplankton for feeding marine invertebrates. In: Smith WL, Chanley MH (eds) Culture of marine invertebrate animals. Plenum Press, New York, p 26–60

Guillard RRL, Ryther JH (1962) Studies of marine planktonic diatoms. I. *Cyclotella nana* Hustedt and *Detonula confervacea* (Cleve). Can J Microbiol 8:229–239

Hartig P, Wolfstein K, Lippemeier S, Colijn F (1998) Photosynthetic activity of natural microphytobenthos populations measured by fluorescence (PAM) and ^{14}C-tracer methods: a comparison. Mar Ecol Prog Ser 166:53–62

Johnson Z, Barber RT (2003) The low-light reduction in the quantum yield of photosynthesis: potential errors and biases when calculating the maximum quantum yield. Photosynth Res 75:85–95

Kaiblinger C, Dokulil MY (2006) Application of fast repetition rate fluorometry to phytoplankton photosynthetic parameters in freshwaters. Photosynth Res 88:19–30

Kana TM (1990) Light-dependent oxygen cycling measured by an oxygen-18 isotope dilution technique. Mar Ecol Prog Ser 64:293–300

Kana TM (1992) Relationship between photosynthetic oxygen cycling and carbon assimilation in *Synechococcus* WH7803 (Cyanophyta). J Phycol 28:304–308

Keller MD, Selvin RC, Claus W, Guillard RRL (1987) Media for the culture of oceanic ultraphytoplankton. J Phycol 23:633–638

Kirk JTO (1994) Light and photosynthesis in aquatic ecosystems, 2nd edn. Cambridge University Press, Cambridge

Kolber ZS, Falkowski PG (1993) Use of active fluorescence to estimate phytoplankton photosynthesis *in situ*. Limnol Oceanogr 38:1646–1665

Kolber ZS, Zehr J, Falkowski PG (1988) Effects of growth irradiance and nitrogen limitation on photosynthetic energy conversion in Photosystem II. Plant Physiol 88:923–929

Kolber ZS, Prášil O, Falkowski PG (1998) Measurements of variable chlorophyll fluorescence using fast repetition rate techniques: defining methodology and experimental protocols. Biochim Biophys Acta 1367:88–106

Krause GH, Weis E (1991) Chlorophyll fluorescence and photosynthesis: the basics. Annu Rev Plant Physiol Plant Mol Biol 42:313–349

Kromkamp JC, Forster RM (2003) The use of variable fluorescence measurements in aquatic ecosystems: differences between multiple and single turnover measuring protocols and suggested terminology. Eur J Phycol 38:103–112

Kromkamp JC, Dijkman NA, Peene J, Simis SGH, Gons HJ (2008) Estimating phytoplankton primary production in Lake IJsselmeer (The Netherlands) using variable fluorescence (PAM-FRRF) and C-uptake techniques. Eur J Phycol 43:327–344

Laws EA (1991) Photosynthetic quotients, new production and net community production in the open ocean. Deep-Sea Res 38:143–167

Lewitus AJ, Kana TM (1995) Light respiration in six estuarine phytoplankton species: contrasts under photoautotrophic and mixotrophic growth conditions. J Phycol 31:754–791

Luz B, Barkan E, Sagi Y, Yacobi YZ (2002) Evaluation of community respiratory mechanisms with oxygen isotopes: a case study in Lake Kinneret. Limnol Oceanogr 47:33–42

MacIntyre HL, Cullen JJ (2005) Using cultures to investigate the physiological ecology of microalgae. In: Andersen RA (ed) Algal culturing techniques. Elsevier Academic Press, Burlington, MA, p 287–326

MacIntyre HL, Geider RJ, McKay RM (1996) Photosynthesis and regulation of Rubisco activity in net phytoplankton from Delaware Bay. J Phycol 32:718–731

MacIntyre HL, Kana TM, Geider RJ (2000) The effect of water motion on short-term rates of photosynthesis by marine phytoplankton. Trends Plant Sci 5:12–17

Mackey KR, Paytan A, Grossman AR, Bailey S (2008) A photosynthetic strategy for coping in a high-light, low-nutrient environment. Limnol Oceanogr 53:900–913

McDonald AE, Vanlerberghet GC (2006) Origins, evolutionary history, and taxonomic distribution of alternative oxidase and plastoquinol terminal oxidase. Comp Biochem Physiol D 1:357–364

Melrose DM, Oviatt CA, O'Reilly JE, Berman MS (2006) Comparisons of fast repetition rate fluorescence estimated primary production and ^{14}C uptake by phytoplankton. Mar Ecol Prog Ser 311:37–46

Moore CM, Suggett DJ, Holligan PM, Sharples J and others (2003) Physical controls on phytoplankton physiology and production at a shelf sea front: a fast repetition-rate fluorometer based field study. Mar Ecol Prog Ser 259:29–45

Moore CM, Suggett DJ, Hickman AE, Kim YN and others (2006) Phytoplankton photoacclimation and photoadaptation in response to environmental gradients in a shelf sea. Limnol Oceanogr 51:936–949

Pemberton KL, Clarke R, Joint I (2006) Quantifying uncertainties associated with the measurement of primary production. Mar Ecol Prog Ser 322:51–59

Pemberton KL, Smith REH, Silsbe GM, Howell T, Watson SB (2007) Controls on phytoplankton physiology in Lake Ontario during the late summer: evidence from new fluorescence methods. Can J Fish Aquat Sci 64:58–73

Prášil O, Kolber Z, Berry JA, Falkowski PG (1996) Cyclic electron flow around photosystem II *in vivo*. Photosynth Res 48:395–410

Quigg A, Kevekordes K, Raven JA, Beardall J (2006) Limitations on microalgal growth at very low photon fluence rates: the role of energy slippage. Photosynth Res 88: 299–310

Raateoja M, Seppälä J, Kuosa H (2004) Bio-optical modelling of primary production in the SW Finnish coastal zone, Baltic Sea: fast repetition rate fluorometry in Case 2 waters. Mar Ecol Prog Ser 267:9–26

Reinfelder JR, Kraepiel AML, Morel FMM (2000) Unicellular C_4 photosynthesis in a marine diatom. Nature 407: 996–999

Raghavendra AS, Padmasree K (2003) Beneficial interactions of mitochondrial metabolism with photosynthetic carbon assimilation. Trends Plant Sci 8:546–553

Roberts K, Garnum E, Leegood RC, Raven JA (2007) C_3 and C_4 pathways of photosynthetic carbon assimilation in marine diatoms are under genetic, not environmental, control. Plant Physiol 145:230–235

Sarma VVSS, Abe O, Hashimoto S, Inhuma A, Saino T (2005) Seasonal variations in triple oxygen isotopes and gross oxygen production in Sagami Bay, central Japan. Limnol Oceanogr 50:544–552

Schreiber U, Neubauer C, Schuwa U (1993) PAM fluorometer based on medium-frequency pulsed Xe-flash measuring light: a highly sensitive new tool in basic and applied photosynthesis research. Photosynth Res 36:65–72

Shoaf WT, Lium BW (1976) Improved extraction of chlorophyll *a* and *b* from algae using dimethyl sulfoxide. Limnol Oceanogr 21:926–928

Smyth TJ, Pemberton KL, Aiken J, Geider RJ (2004) A methodology to determine primary production and phytoplankton photosynthetic parameters from fast repetition rate fluorometry. J Plankton Res 26:1337–1350

Steeman Nielsen E (1952) The use of radioactive carbon (C^{14}) for measuring organic production in the sea. J Cons Int Explor Mer 16:117–140

Suggett DJ, Kraay G, Holligan P, Davey M, Aiken J, Geider RJ (2001) Assessment of photosynthesis in a spring cyanobacterial bloom by use of a fast repetition rate fluorometer. Limnol Oceanogr 46:802–810

Suggett DJ, Oxborough K, Baker NR, MacIntyre HL, Kana TM, Geider RJ (2003) Fast repetition rate and pulse amplitude modulation chlorophyll *a* fluorescence measurements for assessment of photosynthetic electron transport in marine phytoplankton. Eur J Phycol 38:371–384

Suggett DJ, MacIntyre HL, Geider RJ (2004) Evaluation of biophysical and optical determinations of light absorption by photosystem II in phytoplankton. Limnol Oceanogr Methods 2:316–332

Suggett DJ, Maberly SC, Geider RJ (2006a) Gross photosynthesis and lake community metabolism during the spring phytoplankton bloom. Limnol Oceanogr 51:2064–2076

Suggett DJ, Moore CM, Marañón E, Omachi C, Varela RA, Aiken J, Holligan PM (2006b) Photosynthetic electron turnover in the tropical and subtropical Atlantic Ocean. Deep-Sea Res II 53:1573–1592

Suggett DJ, Le Floc'H E, Harris GN, Leonardos N, Geider RJ (2007) Different strategies of photoacclimation by two strains of *Emiliania huxleyi* (Haptophyta). J Phycol 43: 1209–1222

Suggett DJ, Warner ME, Smith DJ, Davey P, Hennige SJ, Baker NR (2008) Photosynthesis and production of hydrogen peroxide by *Symbiodinium* (Pyrrhophyta) phylotypes with different thermal tolerances. J Phycol 44:948–956

Van Heukelem L, Lewitus AJ, Kana TM (1992) High-performance liquid chromatography of phytoplankton pigments using a polymeric reversed-phase C18 column. J Phycol 28:867–872

Wagner H, Jakob T, Wilhelm C (2006) Balancing the energy flow from captured light to biomass under fluctuating light conditions. New Phytol 169:95–108

Weger HG, Birch DG, Elrifi IR, Turpin DH (1988) Ammonium assimilation requires mitochondrial respiration in the light: a study with the green alga *Selenastrum minutum.* Plant Physiol 86:688–692

Weger HG, Herzig R, Falkowski PG, Turpin DH (1989) Respiratory losses in the light in a marine diatom: measurements by short-term mass spectrometry. Limnol Oceanogr 34:1153–1161

Welschmeyer NA (1994) Fluorometric analysis of chlorophyll *a* in the presence of chlorophyll *b* and pheopigments. Limnol Oceanogr 39:1985–1992

Williams PJLeB, Raine RCT, Bryan JR (1979) Agreement between the ^{14}C and the oxygen methods of measuring phytoplankton production: a reassessment of photosynthetic quotient. Oceanol Acta 2:411–416

Xue X, Gautheir DA, Turpin DH, Weger HG (1996) Interactions between photosynthesis and respiration in the green alga *Chlamydomonas reinhardtii.* Plant Physiol 112: 1005–1014

Zhu G, Jensen RG, Bohnert HJ, Wildner GF, Schlitter J (1998) Dependence of catalysis and CO_2/O_2 specificity of Rubisco on the carboxy-terminus of the large subunit at different temperatures. Photosynth Res 57:71–79

Editorial responsibility: Tom Berman, Migdal, Israel

Submitted: December 9, 2008; Accepted: March 18, 2009
Proofs received from author(s): May 27, 2009